Use of Photoaffinity Probes Containing Poly(ethylene glycol) Spacers for Topographical Mapping of the Cholecystokinin Receptor Complex†

Stephen P. Powers, Ivy Foo, Delia Pinon, Ulrich G. Klueppelberg, John F. Hedstrom, and Laurence J. Miller*
Gastroenterology Research Unit, Mayo Clinic, Rochester, Minnesota 55905
Received July 18, 1990; Revised Manuscript Received October 2, 1990

ABSTRACT: To further define the structure of the pancreatic cholecystokinin (CCK) receptor and the topographical distance relationships between its subunits, we developed a series of monofunctional photoaffinity probes in which a fixed receptor-binding domain was separated from a photolabile nitrophenylacetamido group by defined lengths of a flexible spacer. The well-characterized CCK receptor radioligand ^{125}I-D-Tyr-Gly-[(Nle^{28,31})CCK-26-33] provided the receptor-binding component of the probes, while the polymer poly(ethylene glycol) (2, 4, 7, and 10 monomer units long) was used as the spacer. The patterns of affinity labeling of rat pancreatic plasma membranes were examined as a function of spacer length. This ranged from 7.3 to 16.2 Å, as calculated by root-mean-square end-to-end distances and validated experimentally by time-resolved fluorescence resonance energy transfer measurements. All probes in the series specifically labeled the M_r = 85 000–95 000 glycoprotein with M_r = 42 000 core, which has been proposed to contain the hormone recognition site. In addition, when the spacer length reached 16.2 Å, membrane proteins of M_r = 80 000 and M_r = 40 000 were specifically labeled. The product of endo-β-*N*-acetylglucosaminidase F digestion of the M_r = 80 000 protein was M_r = 65 000, similar to a protein previously identified in affinity labeling experiments using a CCK-33-based probe. These observations are consistent with the M_r = 85 000–95 000 pancreatic protein representing the hormone-binding subunit of the CCK receptor, while proteins of M_r = 80 000 and M_r = 40 000 may represent noncovalently associated subunits sited within 16.2 Å of the binding domain. This approach of using flexible, defined-length photolabile probes for the topographical mapping of protein complexes and their domains should be applicable to numerous analogous systems.

It has been assumed that the pancreatic cholecystokinin (CCK) receptor represents a multisubunit complex on the basis of affinity labeling studies which have identified at least two distinct proteins (Rosenzweig et al., 1983; Sakamoto et al., 1983; Madison et al., 1984, 1987; Pearson & Miller, 1987). However, the function of each and their topographical relationship to each other are unclear.

We have previously proposed the hypothesis that one of these pancreatic plasma membrane proteins (M_r = 85 000–95 000) represents the hormone-binding subunit, while another protein (M_r = 80 000) represents a nonbinding subunit or near neighbor (Klueppelberg et al., 1989b). This was based on the observations that the M_r = 85 000–95 000 protein was labeled with probes in which the site of cross-linking was near to or within the carboxyl-terminal heptapeptide which represents the receptor-binding domain of the hormone (Klueppelberg et al., 1989a,b; Powers et al., 1988a), while the M_r = 80 000 protein (variably described to range from M_r = 76 000 to M_r = 95 000) has only been labeled through the amino-terminal region of CCK-33, a long linear distance from this domain (Rosenzweig et al., 1983; Sakamoto et al., 1983; Madison et al., 1984). The independent and distinct nature of these proteins has been well demonstrated by deglycosylation and peptide mapping studies (Rosenzweig et al., 1984; Pearson et al., 1987a).

Because the conformation of CCK-33 as it binds to the receptor is not known, the amino-terminal site of cross-linking may be topographically near to or far from the carboxyl-terminal receptor-binding domain of this hormone. Therefore, to further test our hypothesis of the relationship between the M_r = 85 000–95 000 and M_r = 80 000 proteins and to gain insight into the topographical relationship between these proteins, we designed and synthesized a novel series of photoaffinity labeling probes. The design of these probes was based on the desire to provide a domain which would specifically bind to the CCK receptor with high affinity and a photolabile domain which could be provided at the end of a variable-length flexible spacer. We hoped that this would permit the labeling of all molecules within a given radial distance of the hormone-binding domain of the receptor.

The choice of ^{125}I-D-Tyr-Gly-[(Nle^{28,31})CCK-26-33] as the receptor-binding domain of these probes was based on several properties of this ligand. It is known to bind to CCK receptors with high affinity and specificity (Pearson et al., 1987b). It possesses a nucleophilic α-amino group which is easily acylated and does not thereby modify receptor binding. It has norleucine substitutions for native methionines, making this peptide more resistant to oxidative damage which may occur during chemical synthesis of the probes.

A photolabile nitrophenylacetamido group was used to provide a site for cross-linking. The short-lived species resulting from ultraviolet irradiation of this group are expected to be of general reactivity. Further, it is reactive enough to attach to nearby molecules upon photolysis, yet it is stable enough to be useful under general laboratory conditions. We have previously been quite successful in using a CCK probe containing the nitrophenyl moiety to affinity label the CCK receptor on several target tissues (Powers et al., 1988a;

†This work was supported by Grants DK32878 (L.J.M.) and DK34988 (L.J.M. and S.P.P.) from the National Institutes of Health, the Chadwick Foundation (L.J.M.), Deutsche Forschungsgemeinschaft KL 607/1-1 (U.G.K.), and a Summer Research Fellowship from the American Gastroenterological Association (I.F.).
* Address correspondence to this author at the Center for Basic Research in Digestive Diseases, Guggenheim 17, Mayo Clinic, 200 First St., S.W., Rochester, MN 55905.

0006-2960/91/0430-676$02.50/0 © 1991 American Chemical Society

Schjoldager et al., 1988).

Perhaps the most important element of the series of probes was the flexible spacer. The choice of increasing-length polymers of poly(ethylene glycol) (PEG) was based on several considerations. It has been shown to not perturb the conformation of peptides to which it is attached (Mutter, 1977; Bonora et al., 1978). The polyether structure of the polymer chain possesses amphiphilic characteristics, enhancing solubility in both water and polar organic solvents. In aqueous solution PEG is predicted to act as a freely permeable coil, allowing the attached photolabile group access to the maximum volume of circumambient space. In addition, it has been proposed that PEG facilitates penetration of the membrane lipid bilayer (Naccache & Sha'afi, 1973; Butterworth et al., 1987). This may even permit the identification of receptor-associated proteins which do not reach the extracellular space.

In addition to the synthesis of this family of probes and their application to the topographical mapping of the pancreatic CCK receptor, we have studied the conformational behavior of the PEG spacer in probes such as these. Theoretical end-to-end distances of the PEG series were calculated as root-mean-squares on the basis of statistical polymer theory and the experimentally determined characteristic ratio C_∞ (Kurata et al., 1975). The experimental method of time-resolved fluorescence resonance energy transfer (Amir & Haas, 1987) was applied to the same question, by use of the PEG_{10} polymer with a tryptophan fluorophore on one end and a dansyl acceptor on the other end.

Materials and Methods

Reagents. The starting materials for PEG derivative synthesis, 2-(2-aminoethoxy)ethanol (PEG_2, >95% purity), tetrakis(ethylene glycol) (PEG_4, >95% purity), poly(ethylene glycol) 350 (PEG_7, polydisperse with nominal molecular weight 350), and poly(ethylene glycol) 400 (PEG_{10}, polydisperse with nominal molecular weight 400), were purchased from Aldrich Chemical Co. (Milwaukee, WI). Sodium azide, *p*-toluenesulfonyl chloride, dansyl chloride, and 4-nitrophenylacetic acid were also from Aldrich. Phosgene (20% in toluene) was from Fluka Chemical Corp. (Ronkonkoma, NY). Palladium on 10% activated carbon and tryptophan methyl ester hydrochloride were supplied by Chemical Dynamics Corp. (South Plainfield, NJ). 1-Ethyl-3-[3-(dimethylamino)propyl]carbodiimide (EDC) was from Sigma Chemical Co. (St. Louis, MO). Endo-β-*N*-acetylglucosaminidase F (endo F) was prepared from suspension cultures of *Flavobacterium meningosepticum* (American Type Tissue Culture Association, Rockville, MD) as described by Elder and Alexander (1982).

Analytical Methods. Nuclear magnetic resonance (^1H NMR) spectroscopy was performed on an NR/80 spectrometer (International Business Machines, Danbury, CT). Analytical HPLC was performed on a Beckman reverse-phase column, with 5-μm C-18 packing, 0.46 × 25cm. A linear gradient of 10–60% acetonitrile at a flow rate of 1 mL/min was used. The mobile phase consisted of 0.1 M triethylamine–acetate, pH 5.0.

Synthesis of Photoaffinity Probes. Probes consisted of a photolabile nitrophenylacetamido group separated from a radioiodinated analogue of the CCK receptor-binding domain, ^{125}I-D-Tyr-Gly-[(Nle^{28,31})CCK-26–33], by various-length PEG polymers. Probes nominally containing 2, 4, 7, and 10 monomer units were synthesized. Those with 2 and 4 units were monodisperse, while those with mean lengths of 7 and 10 units were polydisperse.

The general strategy for synthesis of the probes is shown in Scheme I. One terminal hydroxyl group from poly(ethylene glycol) was replaced with the photolabile 4-nitrophenylacetamido function. The second hydroxyl function was then converted to a chloroformate, and the product was used immediately to acylate the previously radioiodinated peptide, ^{125}I-D-Tyr-Gly-[(Nle^{28,31})CCK-26–33].

Scheme I: General Strategy for Probe Synthesis

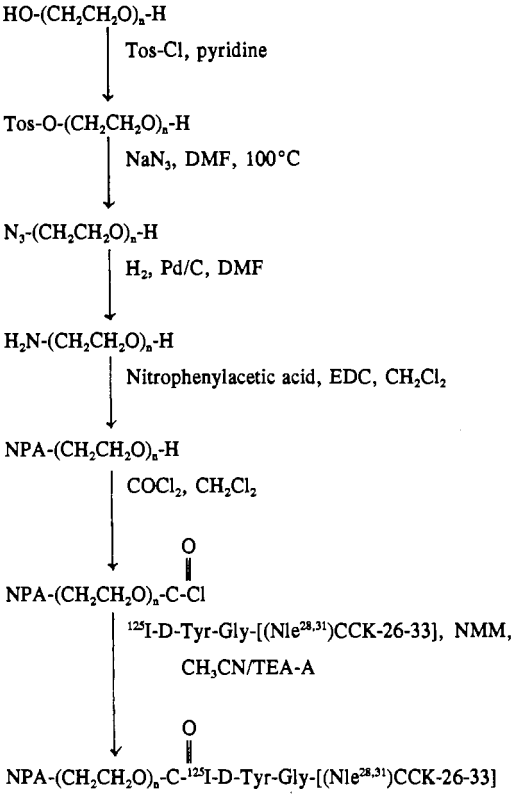

Below, we will describe in detail the synthesis of the PEG_4-based probe. Probes based on PEG_7 and PEG_{10} were prepared similarly, while 2-(2-aminoethoxy)ethanol was the starting material for the probe based on PEG_2. Analytical data for all NPA-PEG derivatives are shown in Table I.

Synthesis of ^{125}I-D-Tyr-Gly-[(Nle^{28,31})CCK-26–33]. The decapeptide ^{125}I-D-Tyr-Gly-[(Nle^{28,31})CCK-26–33] was used as the receptor-binding component of all probes. It has previously been demonstrated to have biological activity and binding characteristics similar to those of native CCK-8 (Pearson et al., 1987), while being resistant to oxidation and possessing an amino group for acylation. This peptide was synthesized by a combination of solid-phase and solution techniques as we described (Powers et al., 1988b). It was iodinated oxidatively with *N*-chloro-benzenesulfonamide (Iodo-Beads, Pierce Chemical Co.) and purified to homogeneity by reversed-phase HPLC (specific radioactivity 2000 Ci/mmol) (Powers et al., 1988b).

Mono-Tos-PEG$_4$. *p*-Toluenesulfonyl chloride (3.81 g, 20 mmol) was reacted with PEG_4 (3.88 g, 20 mmol) in pyridine (30 mL) at room temperature for 3 h. Solvent was removed by rotary evaporation, and the monotosyl derivative was purified by reversed-phase HPLC on a Vydac 218TP152022 column. A 50-min linear gradient from 10 to 60% acetonitrile in water at a flow rate of 10 mL/min was used.

Amino-PEG$_4$. Mono-Tos-PEG_4 (0.98 g, 2.84 mmol) was stirred in DMF (5 mL). Sodium azide (1.3 g, 20 mmol) was added slowly. The reaction was performed in a hot water bath (100 °C) under a stream of N_2 for 2 h. The excess NaN_3 was filtered off, and palladium on 10% activated carbon (500 mg) was added. Hydrogenation was carried out under H_2 at atmospheric pressure overnight. The catalyst was removed by

filtration through Celite 545, and solvent was removed by rotary evaporation.

NPA-PEG$_4$. 4-Nitrophenylacetic acid (0.34 g, 1.88 mmol) was activated with EDC (0.13 g, 1.88 mmol) in CH_2Cl_2 (2 mL) for 10 min in an ice bath before amino-PEG$_4$ (362 mg, 1.88 mmol) in CH_2Cl_2 (1 mL) was added dropwise. After reacting in an ice bath for 4 h, product was purified on a Vydac 218TP152022 column as described above.

Coupling to ^{125}I-D-Tyr-Gly-[(Nle^{28,31})CCK-26–33]. NPA-PEG$_4$ (13.2 mg, 0.042 mmol) was activated with 20% phosgene in toluene (0.23 mL, 0.42 mmol) in CH_2Cl_2 (5 mL) for 2 h in an ice bath. Solvents and excess phosgene were removed under vacuum, and the remaining oil was dissolved in 100 μL of CH_3CN. This solution and 20 μL of *N*-methylmorpholine were added to freshly radioiodinated D-Tyr-Gly-[(Nle^{28,31})-CCK-26–33]. After 1 h, products were purified on a Vydac 218TP54 reversed-phase column. The mobile phase consisted of 0.1 M triethylamine–acetate, pH 5.0, buffer. A 50-min linear gradient from 10 to 60% acetonitrile at a flow rate of 1 mL/min was used. Approximately 10% of radioiodinated peptide was recovered as PEG-acylated product within the relevant peak.

Synthesis of NPA-PEG$_{10}$-^{127}I-D-Tyr-Gly-[(Nle^{28,31})CCK-26–33]. Iodo-D-tyrosine was reacted with 2 mol of [(fluorenylmethyl)oxy]carbonyl chloride (Fmoc-Cl) in 0.2 M Na_2CO_3/dioxane (1:1) for 2 h. Solvents were removed by rotary evaporation, and the residue was washed with ether and 1 N HCl and dried in vacuo. The *N*-succinimidyl ester of bis-Fmoc-^{127}I-D-Tyr was prepared and used to acylate Gly-[(Nle^{28,31})CCK-26–33] as we described previously (Powers et al., 1988b) to give ^{127}I-D-Tyr-Gly-[(Nle^{28,31})CCK-26–33]. This peptide was coupled with NPA-PEG$_{10}$ by activation with phosgene as described above.

Synthesis of Dansyl-PEG$_{10}$-Trp-OMe. Dansyl-PEG$_{10}$-Trp-OMe was prepared from the same precursor amino-PEG$_{10}$ as that used in the synthesis of NPA-PEG$_{10}$-^{127}I-D-Tyr-Gly-[(Nle^{28,31})CCK-26–33] described above. Amino-PEG$_{10}$ (200 mg, 0.5 mmol) in CH_2Cl_2 (1 mL) was treated with dansyl chloride (161 mg, 0.6 mmol) at 25 °C for 12 h. The dansyl-PEG$_{10}$ derivative was immediately activated with phosgene solution (0.5 mL, 0.91 mmol) for 1 h in an ice bath. Solvent and excess phosgene were removed under vacuum, and tryptophan methyl ester hydrochloride (255 mg, 1 mmol) and triethylamine (139 μL, 1 mmol) in 2 mL of DMF were added. After 2 h, the product was purified on a Vydac 218TP1010 reversed-phase column. The mobile phase consisted of 0.1 M triethylamine–acetate, pH 5.0, buffer. A 50-min linear gradient from 10 to 60% acetonitrile at a flow rate of 4 mL/min was used. ^{252}Cf plasma desorption mass spectrometry showed the same polydisperse pattern observed for NPA-PEG$_{10}$-^{127}I-D-Tyr-Gly-[(Nle^{28,31})CCK-26–33] with the most abundant oligomer containing PEG$_{10}$.

Fluorescence Resonance Energy Transfer Measurements. The photolabile NPA group and ^{125}I-D-Tyr-Gly-[(Nle^{28,31})-CCK-26–33] of the longest affinity labeling probe were replaced with dansyl (DNS) and tryptophan methyl ester, respectively, and time-resolved fluorescence resonance energy transfer techniques (Amir & Haas, 1987) were used to experimentally determine the end-to-end length of PEG$_{10}$. Tryptophan fluorescence lifetimes were measured by the method of time-correlated single photon counting on an instrument we have described previously (Hedstrom et al., 1988).

Data analysis was performed with Globals Unlimited software. Initially, the undansylated PEG$_{10}$-tryptophan lifetime was fit to a biexponential decay function. The recovered parameters (preexponential factor and decay rate) were input as fixed variables in the DNS-PEG$_{10}$-Trp fluorescence decay parameter sets. The model function was adjusted to recover either a discrete or a Gaussian-distributed distance for this species. Analysis of the reduced χ^2 value and the autocorrelation trace of the residuals determined the proper function to describe the PEG conformation in solution.

Photoaffinity Labeling. Pancreatic membranes were prepared from 125–150-g male Harlan Sprague-Dawley rats (Pearson & Miller, 1987). Binding was performed with 50 μg of rat pancreatic membrane by use of 375 pM radiolabeled probe in 1 mL of buffer containing 50 mM MES, pH 6.0, 130 mM NaCl, 7.7 mM KCl, 5 mM $MgCl_2$, 1 mM EGTA, 1 mM KH_2PO_4, 0.5 mM phenylmethanesulfonyl fluoride, 0.01% soybean trypsin inhibitor, and 0.2% bovine serum albumin (BSA). Binding was performed in the presence or absence of competing CCK-8 (0.1 μM) to determine specific labeling. The suspensions were allowed to incubate at 24 °C for 60 min, when 0.5 mL of iced buffer was added and bound and unbound ligand were separated by centrifugation at 10000*g* for 5 min. The membrane pellets were resuspended at 4 °C in 1 mL of protein-free buffer and transferred to borosilicate glass tubes for photolysis. This was performed at 4 °C in a Rayonet Model RP-100 photolysis apparatus (Southern New England Ultraviolet, Hamden, CT) at a distance of 5.7 cm, with ultraviolet light having a mean wavelength of 300 nm.

After photolysis, membranes were pelleted by centrifugation for 5 min at 10000*g* and solubilized in sample buffer containing 4% sodium dodecyl sulfate (SDS), 10 mM EDTA, 15% sucrose, 0.01% bromophenol blue, and 1.25 M Tris (pH 6.8) with 0.1 M dithiothreitol. These samples were electrophoresed on 10% SDS–polyacrylamide gels under the conditions described by Laemmli (1970). The gels were frozen and exposed to X-ray film (Kodak XAR-5) at −70 °C for 1–14 days with a Du Pont Quanta III intensifying screen. The molecular weight standards used were myosin (M_r = 200 000), β-galactosidase (M_r = 116 500), phosphorylase B (M_r = 92 500), BSA (M_r = 66 000), ovalbumin (M_r = 45 000), and carbonic anhydrase (M_r = 29 000). The M_r values for the photoaffinity-labeled proteins were calculated from a plot of log M_r versus mobility of the standard proteins.

Deglycosylation Using Endo F. The specifically affinity-labeled regions of the gels were cut out and divided into slices. Each gel slice was then placed into an electroelution chamber (ISCO Model 1750 electrophoretic concentrator, Lincoln, NE) with cellulose dialysis membranes having a molecular cutoff at M_r = 3500. This contained 0.01 M Tris–acetate and 0.1% NP40 at pH 8.6 in the inner chamber and 0.04 M Tris–acetate and 0.1% NP40 at pH 8.6 in the outer chamber. Elution was performed at 3 W for 24 h. The electroeluted solution was mixed at a 1:1 ratio (v/v) with endo F medium (0.1 M sodium phosphate, pH 6.1, containing 50 mM EDTA, 0.1% NP40, 0.1% SDS, and 1% 2-mercaptoethanol) to give a final pH of 6.2. Three units of endo F was added, and this was allowed to digest at 37 °C for 12 h. The sample was diluted in an equal volume of sample buffer and analyzed with convex 5–20% gradient gels. The gels were stained with Coomassie Brilliant Blue, dried, and exposed to X-ray film (Kodak XAR-5) at −70 °C for 14–30 days with Du Pont Quanta III intensifying screens. The M_r values of products were determined by interpolation among standard proteins.

RESULTS

Synthesis of Topographical Probes. Each of the probes was synthesized according to the procedure described above. The degree of polymerization of each PEG spacer was assessed by

Table I: Characterization of NPA-PEG Products

	NMR data[a]	HPLC (retention time, min)[b]	yield (%)[c]
NPA-PEG_2	2	15.1	8
NPA-PEG_4	4	18.6	30
NPA-PEG_7	7	21.9	9
NPA-PEG_{10}	20[d]	24.1	28

[a] Ratio of methylene (PEG) to aryl protons (NPA). [b] Retention time is of monodisperse products, or for compounds which were polydisperse retention time given represents that of the most abundant oligomer. [c] Percentage of mono-Tos-PEG derivative yielding NPA product. [d] Extra protons likely due to retained water, difficult to remove from longer PEG polymers.

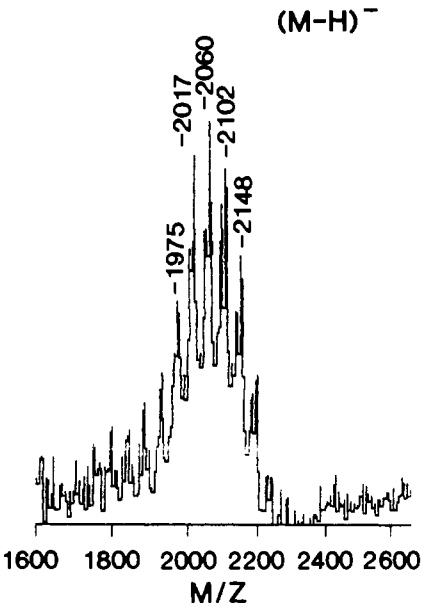

FIGURE 1: Negative ion mode californium-252 plasma desorption mass spectrum of the ^{127}I-labeled analogue of the PEG_{10}-based CCK receptor probe. A range of molecular ions correspond with the polydisperse NPA-PEG_{10} used in its synthesis. The labeled values on the figure represent m/z of each respective peak. The ion species with m/z 2102 corresponds to the calculated $(M - H)^-$ of 2100.0 for the PEG_{10} species. Peaks differ by an average of 43.3 mass units (theoretical for series of PEG polymers is 44).

NMR and HPLC (Table I). NPA-PEG_2 and NPA-PEG_4 were single, defined species, while NPA-PEG_7 and NPA-PEG_{10} were polydisperse, similar to their starting materials. NPA-PEG_{10} had an average degree of polymerization of n = 10 and >75% mole fraction distributed from n = 8 to n = 12.

After acylation of the CCK peptides, the radiolabeled probes in each case eluted as single peaks on HPLC. These, however, continued to reflect the polydisperse nature of the NPA-PEG used in their synthesis, as demonstrated by the range of molecular ions observed in californium desorption mass spectrometry of the ^{127}I-labeled analogue of the PEG_{10}-based CCK receptor probe (Figure 1).

Theoretical and Experimental Dimensions of Spacers. The theroretical mean-square end-to-end distance for an ideal, completely flexible, and volumeless polymer of n atoms with bond length l between atoms is

$$r^2 = nl^2$$

This, however, ignores steric hindrance, restricted bond geometry, excluded volume, and solvation effects. Taking these factors into account and assuming that the buffers used conform to Flory or θ conditions, the above expression becomes

$$r^2 = C_\infty nl^2$$

Table II

PEG units	extended length (Å)	calculated r_{rms} length (Å)	experimentally derived length (Å)
2	7.2	7.3	
4	14.4	10.3	
7	25.2	13.6	
10	36.0	16.2	18.0

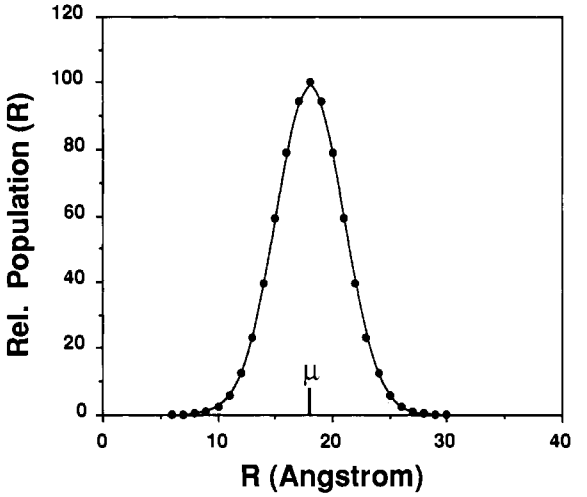

FIGURE 2: Gaussian distribution curve for DNS to Trp distances for DNS-PEG_{10}-Trp-OMe in aqueous solution. The mean separation μ between chromophores is 18 Å, with fwhm of 7 Å, on the basis of time-resolved fluroescence resonance energy transfer measurements.

For PEG in θ solvents the experimentally determined characteristic ratio C_∞ is 4.1 (Kurata et al., 1975). By use of this value and a skeletal bond length of 1.46 Å, the root-mean-square end-to-end distances, r_{rms}, for the different PEG polymers were calculated (shown in Table II).

A distribution of end-to-end distances is expected for PEG spacers because of their high degree of flexibility. The experimental distribution function for PEG_{10} determined from time-resolved fluorescence resonance energy transfer measurements reflects this and is plotted in Figure 2. The most probable distance value determined experimentally is also shown in Table II. This shows that the calculated theoretical and experimentally derived distance values agree quite nicely.

Photoaffinity Labeling. The intensity of specific labeling of pancreatic membrane proteins was dependent upon the duration of exposure to ultraviolet light, with more intense labeling occurring with longer exposures (Figure 3). Figure 4 demonstrates that the labeling was inhibited in a concentration-dependent manner by the presence of competing CCK-8 in the incubation medium. This effect was similar for probes with short (PEG_4) and long (PEG_{10}) spacers. Figure 4 shows the specific labeling of a band in the same region of the gel by each of the probes, independent of spacer length. This labeling includes the same region of the gel as the M_r = 85 000–95 000 band previously reported with a series of CCK receptor probes and felt to represent the best candidate for the hormone-binding subunit (Pearson & Miller, 1987; Klueppelberg et al., 1989a,b; Powers et al., 1988a). However, the band labeled by these probes was even more broad and poorly resolved than the glycoprotein band previously described. The PEG may have interfered with SDS binding to the protein, and thereby affect migration on the gel in a similar way that carbohydrate affects resolution and migration. The way to be certain that it indeed represented the same protein was by deglycosylation with endo F. Those results follow. In addition, only when the spacer length reached 10 monomer

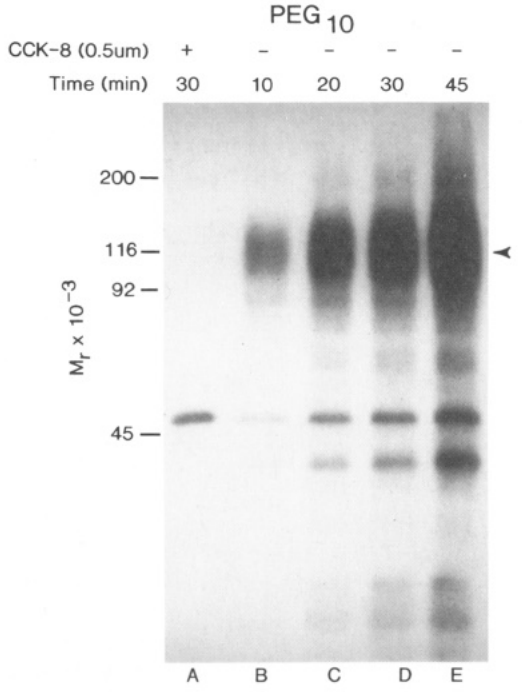

FIGURE 3: Time course of photoaffinity labeling of pancreatic membranes. Membranes were incubated with 375 pM NPA-PEG_{10}-^{125}I-D-Tyr-Gly-[($Nle^{28,31}$)CCK-26–33] with or without 0.1 μM CCK-8 and photolyzed for the indicated times. Specific labeling was evident in the region of the CCK receptor (arrowhead) at 10 min and continued to increase with photolysis times up to 45 min.

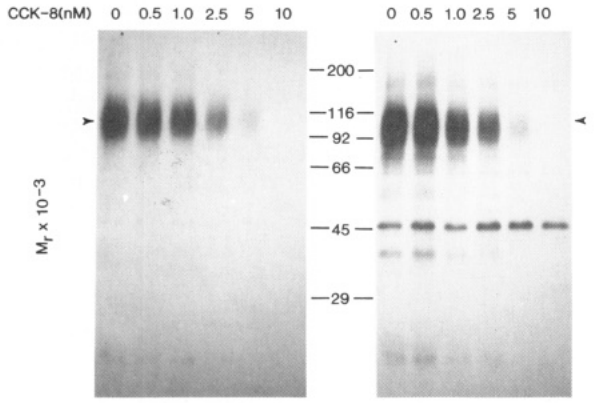

FIGURE 4: Inhibition of photoaffinity labeling by native ligand. Membranes were incubated with 375 pM NPA-PEG_4-^{125}I-D-Tyr-Gly-[($Nle^{28,31}$)CCK-26–33] (left) or NPA-PEG_{10}-^{125}I-D-Tyr-Gly-[($Nle^{28,31}$)CCK-26–33] (right) in the presence of increasing concentrations of CCK-8. Photolysis was performed for 30 min. CCK-8 competed for covalent labeling of the major band which includes the M_r = 85 000–95 000 region previously reported (arrowhead), in a concentration-dependent manner, with more than 50% of labeling inhibited by 1 nM CCK-8. Inhibition of labeling of two additional bands at M_r = 80 000 and M_r = 40 000 is also evident when the longer spacer was used (right).

units (r_{rms} of 16.2 Å) did the specifically labeled M_r = 80 000 species appear, as confirmed by its product of deglycosylation (data below). For each of these bands, greater than half of the specific labeling was inhibited by 1 nM CCK-8.

Deglycosylation with Endo F. The labeled, native glycosylated forms of the M_r = 85 000–95 000 and M_r = 80 000 proteins can often appear to overlap with each other when analyzed by SDS–PAGE, but their products of endo F deglycosylation (M_r = 42 000 and M_r = 65 000, respectively) are clearly separated. We therefore divided the affinity labeled regions into slices, electroeluted the contents of each slice, and treated the electroeluted contents with endo F. The deglycosylated products were then reanalyzed by SDS–polyacrylamide gel electrophoresis. The results are shown in Figures 5 and 6. None of the slices from labeling using probes containing PEG_4 or PEG_7 spacers showed a band in the region of M_r = 65 000. For the PEG_{10} probe, the top slices yielded a primary deglycosylation product of M_r = 42 000. The bottom slice, however, yielded a sharp, specific band at M_r = 65 000, as well as a band at M_r = 42 000. Indeed, this is consistent with the endo F deglycosylation product of the M_r = 80 000 glycoprotein previously observed (Klueppelberg et al., 1989b; Rosenzweig et al., 1984).

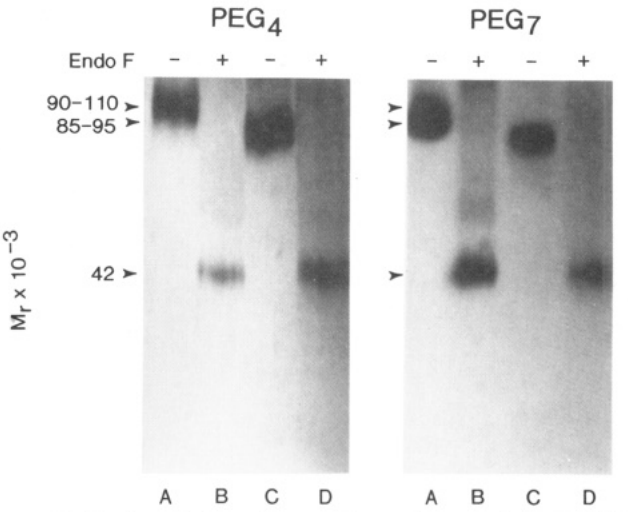

FIGURE 5: Deglycosylation of pancreatic membrane proteins labeled by NPA-PEG_4-^{125}I-D-Tyr-Gly-[($Nle^{28,31}$)CCK-26–33] (left) and NPA-PEG_7-^{125}I-D-Tyr-Gly-[($Nle^{28,31}$)CCK-26–33] (right). The specifically labeled major bands were cut into upper and lower slices, electroeluted, and rerun without treatment (lanes A and C) or after deglycosylation with endo F (lanes B and D). The known M_r = 42 000 deglycosylation product of the M_r = 85 000–95 000 protein was the only product evident in each reaction.

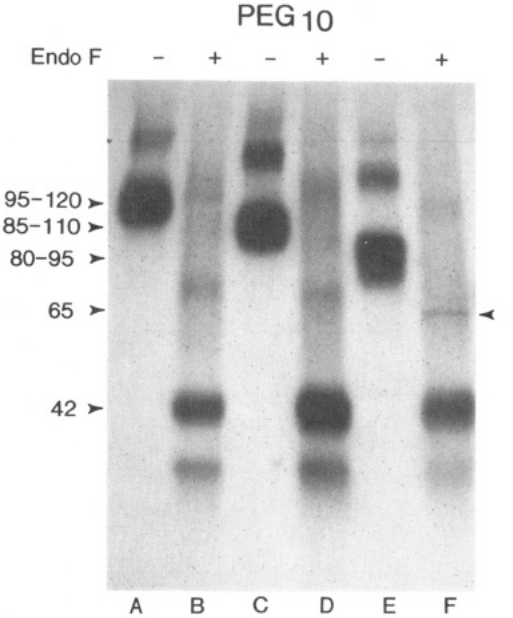

FIGURE 6: Deglycosylation of pancreatic membrane proteins labeled by NPA-PEG_{10}-^{125}I-D-Tyr-Gly-[($Nle^{28,31}$)CCK-26–33]. The specifically labeled region of the gel was cut into three slices, electroeluted, and rerun without treatment (lanes A, C, and E) or after deglycosylation with endo F (lanes B, D, and F). A major deglycosylation product of M_r = 42 000 is evident in lanes B, D, and F, but a sharp band of approximate M_r = 65 000 (arrowhead), typical of that derived from the M_r = 80 000 receptor-associated protein (Rosenzweig et al., 1984), is observed in lane F, derived from the lower slice.

Discussion

Previous studies have suggested that the pancreatic CCK receptor consists of a hormone-binding subunit of M_r = 85000–95000 which is labeled both by "short", CCK-8-based probes and by "long", CCK-33-based probes and a second subunit (M_r = 80000) which is labeled only by the "long" probes. Because the conformation of CCK-33 is not known and because the location of cross-linking on the probe is not well-defined (Lys^1 and Lys^{11} are both possibilities), it has been difficult to infer distance relationships between the two proteins labeled with this ligand. We postulated that a series of photoaffinity probes capable of labeling molecules at increasing distances from the ligand-binding site would first label the M_r = 85000–95000 protein and then, when the effective labeling radius became long enough, would also label the M_r = 80000 protein. The labeling radius at which this transition occurred would approximate the distance between the two subunits. We constructed the required series of photoaffinity probes using PEG spacers to connect a photolabile 4-nitrophenylacetamido group to the CCK receptor ligand, ^{125}I-D-Tyr-Gly-[($Nle^{28,31}$)CCK-26–33].

The 4-nitrophenylacetamido function was chosen as the photolabile component of the probes because our previous experience with nitrophenyl-based probes (Powers et al., 1988) demonstrated adequate efficiency of labeling the CCK receptor (1.4% of specifically bound counts covalently incorporated), with stability to reducing agents and ambient light superior to that of alternatives such as the aryl azide group. The photochemistry of the 4-nitrophenyl alkyl group is not well understood. Photolysis may proceed via a multiphoton process yielding a long-lived triplet state with the capture of the first photon and dissociative decay to radical intermediates with the capture of a second photon (Escher & Guillemette, 1978). The chemistry is likely different from that of the nitroanisoles, which undergo photoactivated aromatic substitution with loss of the methoxy group, since an analogous reaction in the probes described here would result in loss of the radiolabeled portion of these molecules.

Polymeric "spacers" have been used to study the topology of other multimeric protein complexes. Green in 1971 coupled polymethylenediamides to biotin in order to determine the arrangement of subunits in avidin (Green et al., 1971). Butterworth et al. (1987) used varying lengths of PEG polymers to measure the depth of local anesthetic binding sites, and Ruoho and Hall used oligomers of cardiotonic glycosides for mapping (Na,K)-ATPase (Ruoho & Hall, 1980).

PEG has several advantages over other types of potential spacers. Strong precedent exists for the claim that it will not affect the conformation of the peptide to which it is attached (Mutter, 1977; Bonora et al., 1978). Its solubility is ideal for use in aqueous media. Also, it appears to exist as a freely permeable coil in aqueous solution, thus maximizing chances that an appropriate conformation for labeling a neighboring protein can be achieved irrespective of the orientation of such a protein relative to the site of ligand binding. In addition, the root-mean-square end-to-end distances of PEG polymers are readily calculated.

Assuming that θ conditions apply, the root-mean-square end-to-end distances for the PEG chains used in this work range from 7.3 to 16.2 Å. The assumption of θ conditions is an approximation, since the θ temperature in H_2O for PEG is 40 °C, while affinity labeling experiments were performed at 4 °C. However, water is a good solvent for PEG. This and the fact that the characteristic ratio C_∞ has a negative temperature coefficient suggest that any deviation from ideal distribution of conformers would be expected to result in larger values of r_{rms}. Thus, the r_{rms} values shown in Table I can be taken as lower approximations, while the lengths shown for the fully extended conformations are upper limits for the labeling radii of the probes. This range is in good agreement with the value determined experimentally by time-resolved fluorescence resonance energy transfer for PEG_{10}.

A disadvantage to the use of highly flexible spacers is that the volume of space accessible to the photolabile nitrophenyl group increases in proportion to the cube of the radius. The further a protein molecule lies from the binding site of CCK, the smaller the percentage of the total accessible volume it represents, theoretically resulting in lower efficiency of labeling. This effect is important if the radius is large, but it should produce only a 4-fold difference in labeling efficiency for probes based on PEG_4 and PEG_{10}, respectively ($[10.3/16.2]^3$ = 0.26).

A potential disadvantage to the use of PEG, which has long been known to interact with cell membranes, is the possibility of nonspecific labeling of abundant membrane proteins. The intense nonspecific labeling of a band at M_r = 46000, which is not abolished in the presence of excess unlabeled CCK, could represent such an effect. This was the only species to demonstrate such intense nonspecific labeling, suggesting that this effect does not detract from the utility of the method.

As predicted, the short spacers with r_{rms} of 7.3–13.6 Å labeled only the hormone-binding subunit of the CCK receptor complex upon photolysis. However, when a longer spacer of r_{rms} = 16.2 Å was used, the M_r = 80000 protein previously identified with a CCK-33-based probe was also specifically labeled. Although inhibition of labeling of this protein by competing CCK-8 demonstrated that is was indeed associated with the CCK receptor, a functional role for it in such a complex has not been demonstrated. These data suggest that the M_r = 80000 glycoprotein resides in the plasma membrane with accessible domains likely further than 10 Å and within 16 Å of the site of binding of CCK on the M_r = 85000–95000 protein. In addition, a M_r = 40000 protein was specifically labeled with the probe containing the PEG_{10} spacer, at the same time that the M_r = 80000 protein was labeled. This may represent a similarly-sized protein previously also observed (although less consistently than the M_r = 80000 protein) with CCK-33-based affinity labeling (Rosenzweig et al., 1983; Madison et al., 1984).

The approach used in this work toward the investigation of receptor topography has been shown to be very successful in the structural characterization of the pancreatic CCK receptor. These probes will also be quite useful for the analogous characterization of other receptors for this family of hormones. Similarly, this approach of using flexible, defined-length photolabile probes should be useful for the topographical mapping of other protein complexes and their domains.

Acknowledgments

We thank Elizabeth Hadac for excellent technical assistance and Marilyn LeQve for assistance in manuscript preparation.

Registry No. Mono-Tos-PEG_4, 77544-60-6; PEG_4, 25322-68-3; amino-PEG_4, 86770-74-3; NPA-PEG_4, 130700-37-7; NPA-PEG_4-D-TyrGly[$Nle^{28,31}$]CCK(26–33), 130727-30-9; NPA-PEG_7-D-Tyr-Gly[$Nle^{28,31}$]CCK(26–33), 130759-84-1; NPA-PEG_{10}-D-Tyr-Gly-[$Nle^{28,31}$]CCK(26–33), 130727-31-0; NPA-PEG_2-D-Tyr-Gly-[$Nle^{28,31}$]CCK(26–33), 130727-32-1; dansyl-PEG_{10}-Trp-OMe, 130727-33-2; *p*-toluenesulfonyl chloride, 98-59-9; 4-nitrophenylacetic acid, 104-03-0; dansyl chloride, 605-65-2.

References

Amir, A., & Haas, E. (1987) *Biochemistry 26*, 2162–2175.

Bonora, G. M., Toniolo, C., & Mutter, M. (1978) *Polymer 19*, 1382-1386.
Butterworth, J. F., IV, Moran, J. R., Whitesides, G. M., & Strichartz, G. R. (1987) *J. Med. Chem. 30*, 1295-1302.
Elder, J. H., & Alexander, S. (1982) *Proc. Natl. Acad. Sci. U.S.A. 79*, 4540-4544.
Escher, E. H. F., & Guillemette, G. (1978) *J. Med. Chem. 22*, 1047-1050.
Green, N. M., Konieczny, L., Toms, E. J., & Valentine, R. C. (1971) *Biochem. J. 125*, 781-791.
Hedstrom, J., Sedarous, S., & Prendergast, F. G. (1988) *Biochemistry 27*, 6304-6308.
Klueppelberg, U. G., Gaisano, H. G., Powers, S. P., & Miller, L. J. (1989a) *Biochemistry 28*, 3463-3468.
Klueppelberg, U. G., Powers, S. P., & Miller, L. J. (1989b) *Biochemistry 28*, 7124-7129.
Kurata, M., Tsunashima, Y., Iwama, M., & Kamada, K. (1975) in *Polymer Handbook*, 2nd ed. (Brandrup, J., & Immergut, E. H., Eds.) pp iv, 1-iv, 45, Wiley & Sons, New York.
Laemmli, U. K. (1970) *Nature 227*, 680-685.
Madison, L. D., Rosenzweig, S. A., & Jamieson, J. D. (1984) *J. Biol. Chem. 259*, 14818-14823.
Madison, L. D., Jamieson, J. D., & Rosenzweig, S. A. (1987) *Biochem. Biophys. Res. Commun. 143 (2)*, 761-767.
Mutter, M. (1977) *Macromolecules 10*, 1413-1414.
Naccache, P., & Sha'afi, R. I. (1973) *J. Gen. Physiol. 62*, 714-736.
Pearson, R. K., & Miller, L. J. (1987) *J. Biol. Chem. 262*, 869-876.
Pearson, R. K., Miller, L. J., Hadac, E. M., & Powers, S. P. (1987a) *J. Biol. Chem. 262*, 13850-13856.
Pearson, R. K., Powers, S. P., Hadac, E. M., Gaisano, H., & Miller, L. J. (1987b) *Biochem. Biophys. Res. Commun. 147*, 346-353.
Powers, S. P., Fourmy. D., Gaisano, H., & Miller, L. J. (1988a) *J. Biol. Chem. 263*, 5295-5300.
Powers, S. P., Pinon, D. I., & Miller, L. J. (1988b) *Int. J. Pept. Protein Res. 31*, 429-434.
Rosenzweig, S. A., Miller, L. J., & Jamieson, J. D. (1983) *J. Cell Biol. 96*, 1288-1297.
Rosenzweig, S. A., Madison, L. D., & Jamieson, J. D. (1984) *J. Cell Biol. 99*, 1110-1116.
Ruoho, A. E., & Hall, C. C. (1980) *Ann. N.Y. Acad. Sci. 346*, 90-103.
Sakamoto, C., Goldfine, I. D., & Williams, J. A. (1983) *J. Biol. Chem. 258*, 12707-12711.
Schjoldager, B., Powers, S. P., & Miller, L. J. (1988) *Am. J. Physiol. 255*, G579-G586.

Purification and Properties of a Membrane-Bound Insulin Binding Protein, a Putative Receptor, from *Neurospora crassa*†

Hemanta K. Kole, Ganapathy Muthukumar, and John Lenard*

Department of Physiology and Biophysics, University of Medicine and Dentistry of New Jersey, Robert Wood Johnson Medical School, 675 Hoes Lane, Piscataway, New Jersey 08854-5635

Received July 26, 1990; Revised Manuscript Received October 5, 1990

ABSTRACT: The protein that is responsible for specific, high-affinity binding of insulin to the surface of *Neurospora crassa* cells has been purified to homogeneity. The insulin binding activity of solubilized plasma membranes resembled that of intact cells with regard to affinity of binding, specificity for mammalian insulins, and amount of insulin bound per cell. Insulin binding activity was purified from Triton X-100 solubilized membranes in two steps: FPLC on a MonoQ HR5/5 column; and affinity chromatography on insulin-agarose. The pure material migrated as a single band of ca. 66 kDa on SDS gels, pI = 7.4 by isoelectric focusing. The protein bound 5.34 pmol of insulin/μg, or 35% of that expected for univalent binding. Cross-linking of ^{125}I-insulin to pure protein or to solubilized membranes revealed a single labeled band of 67-70 kDa on SDS gels. In nonreducing native gels, two labeled bands of ca. 55 and 110 kDa were produced after cross-linking, and two bands of similar molecular weight bound iodinated insulin after transfer to nitrocellulose filters. These may correspond to active monomer and dimer forms. The pure protein possessed no protein kinase activity against itself, or against exogenous substrates (histone H_2, casein, or the synthetic peptide Glu^{80}-Tyr^{20}), and possessed no detectable phosphorylated amino acids. It is suggested, however, that this 66-kDa protein is the "receptor" that mediates insulin-induced downstream metabolic effects.

Previous reports from this laboratory have documented several metabolic effects of mammalian insulin upon *Neurospora crassa* cells: enhanced production of glucose metabolites including CO_2, ethanol, alanine, and glycogen; enhanced growth and improved viability; and enhanced accumulation of intracellular sodium upon addition of glucose (Fawell et al., 1988; Greenfield et al., 1988, 1990; McKenzie et al., 1988). These observations were of special interest in the light of numerous findings by others that a biologically active insulin-like molecule was found in several different microbial eukaryotes (LeRoith et al., 1980, 1985), in insects, invertebrates, and plants (Collier et al., 1987; Conlon et al.,

†Supported by Grant DK39502 from the National Institutes of Health.
*To whom correspondence should be addressed.

0006-2960/91/0430-682$02.50/0 © 1991 American Chemical Society